I&EC research
Industrial & Engineering Chemistry Research

Article

pubs.acs.org/IECR

Dynamic Modeling and Parameter Estimation for Unit Operations in Lignocellulosic Bioethanol Production

M. Susana Moreno,* Federico E. Andersen, and M. Soledad Díaz

Planta Piloto de Ingeniería Química (PLAPIQUI), CONICET—Universidad Nacional del Sur, Camino La Carrindanga km 7, 8000 Bahía Blanca, Argentina

ABSTRACT: During the past decades, intensive research has been pursued on the development of kinetic models to predict process behavior in ethanol production from lignocellulose. These models comprise a large number of parameters which have to be tuned with appropriate experimental data. Therefore, the parameter estimation problem plays an essential role. This work addresses the parameter estimation problem in models representing dilute acid hydrolysis, detoxification, and cofermentation operations in the biochemical production of ethanol from lignocellulosic biomass. The models are represented by sets of differential-algebraic equations (DAEs). Unlike previous approaches, these models account for the main process variables that affect the entire process, specially the final production of bioethanol. These detailed kinetic models, systematically tuned with experimental data, can be used in future studies within a model-based framework that allows performing realistic simulation and optimization aimed at bioethanol process design. A sensitivity analysis has been performed in order to identify the most sensitive parameters. The parameter estimation problem is solved with a simultaneous optimization approach in which the system of dynamic equations is converted into a set of algebraic ones through orthogonal collocation on finite elements. Thus, estimating the model parameters entails optimizing a weighted least squares objective function subject to the discretized algebraic constraints, resulting in a large-scale nonlinear programming problem (NLP). A good agreement with available experimental data has been obtained with estimated kinetic parameters in each model.

1. INTRODUCTION

Lignocellulosic biomass in nature is by far the most abundant and low-cost feedstock for the production of the so-called second generation biofuels. Furthermore, these biofuels have the potential to replace first generation ones, thus avoiding the controversies resulting from the use of food crops for transport fuel production.

Lignocellulosic materials, such as agricultural and forest residues, or dedicated energy crops, contain a heterogeneous mixture of biopolymers from plant cell walls: cellulose, hemicellulose, and lignin. The remaining small fraction comprises extractives, acids, salts, and minerals. The carbohydrate polymers, i.e., cellulose and hemicelluloses, are a potential source of fermentable sugars (mainly glucose and xylose), but they are within an intricate structure that is recalcitrant to deconstruction.

Lignocellulosic ethanol is one of the major second generation biofuels, and a considerable amount of research is being done in order to develop appropriate technologies for achieving large conversions through biochemical processes.[1−4] One of the major barriers to the economical production of bioethanol is the aforementioned recalcitrance of lignocellulosic raw materials. Their direct bioconversion to ethanol requires a pretreatment stage intended to remove lignin and hydrolyze hemicelluloses. This operation makes cellulose macromolecules more accessible for enzymes, allowing the production of fermentable sugars (glucose) in a further enzymatic hydrolysis stage. In the downstream microbial fermentation, the sugars extracted from celluloses and hemicelluloses are converted to ethanol.

Although different pretreatment techniques have been proposed,[5−7] dilute acid hydrolysis is preferred for industrial applications due to its simplicity and high sugar yield from hemicelluloses.[8,9] Due to the low acid concentrations involved, their recovery may not be required. However, this process presents some disadvantages such as the formation of large amounts of toxic compounds, such as furfural and 5-hydroxymethylfurfural (HMF), generated by degradation of sugars, which can be inhibitory to microorganisms in the downstream fermentation process, with consequent lower ethanol productivities.[10,11] Therefore, an additional operation known as detoxification or conditioning is required after this pretreatment where the toxic materials are converted into less inhibitory components.

A number of kinetic models for the hydrolysis, detoxification, and fermentation operations involved in the production of bioethanol have been reported in the literature.[12−14] However, most of them do not include process variables such as operating temperatures and concentrations of inhibitory compounds that would allow evaluating their influence through simulation and optimization studies. In this way, the developed model can be used in future studies within an optimization framework to determine, for example, whether a detoxification step is required for enhancing yields in the cofermentation process (without the inhibitory compounds removed in the overliming process).

In this work we focus on the parameter estimation of kinetic models considering the main process variables for the unit operations of hydrolysis, detoxification, and fermentation in a bioethanol production plant. More specifically, we aim at identifying realistic dynamic models for the dilute acid hydrolysis, the

Received: September 2, 2012
Revised: February 7, 2013
Accepted: February 16, 2013
Published: February 17, 2013

dx.doi.org/10.1021/ie302358e | *Ind. Eng. Chem. Res.* 2013, 52, 4146−4160

detoxification by addition of $Ca(OH)_2$ (overliming), and the simultaneous fermentation of mixtures of glucose and xylose (cofermentation).

We have extended the model proposed by Lavarack et al.[12] for the dilute acid hydrolysis with the inclusion of kinetic equations for acetic acid and HMF generation. The model also includes the production of xylose, glucose, furfural, and soluble lignin, considering the influence of temperature, acid concentration, and solid to liquid ratio. Regarding the overliming process, sugars and furans generate transient complexes with calcium ions which are degraded to different products. We propose a model based on that of Purwadi et al.[13] in which we have included reaction rates based on the Arrhenius equation to account for the influence of the temperature. Furthermore, we include a new expression for determining the initial concentration of the calcium cation related to the pH level. In the cofermentation operation we have extended the unstructured model developed by Leksawasdi et al.[14] by including new factors that account for furfural toxicity. We propose a first-order kinetics with respect to furfural and biomass concentration for representing the conversion of furfural by a fermentative microorganism.

We formulate the dynamic parameter estimation problem for the above-mentioned models within a simultaneous framework, in which the differential algebraic equation (DAE) system is discretized using orthogonal collocation on finite elements.[15−17] Thus, the DAE constrained optimization problems are transformed into large-scale nonlinear programming (NLP) problems using a weighted least squares objective function. The resulting NLP formulation is then solved with an interior point (IP) program IPOPT[18] that uses full space sequential quadratic programming (SQP) techniques within GAMS.[19]

Prior to parameter estimation, we carry out local sensitivity analysis on each system to determine the set of most influential parameters.[20]

In order to accomplish parameter estimation, the experimental data from Cassales et al.,[21] Purwadi et al.,[13] and Gutierrez-Padilla and Karim[22] are used for hydrolysis, overliming, and fermentation processes, respectively. We determine the main unknown kinetic parameters such as activation energies, pre-exponential factors in the dilute acid hydrolysis and detoxification operations, and the maximum overall specific growth rate and inhibition factors for the fermentation process.

This paper is organizated as follows. Section 2 defines a general estimation problem in DAE models and describes the methodology used for assessing the most influential parameters and the approach for solving the resulting DAE optimization problem. Section 3 describes the proposed models for dilute acid hydrolysis, detoxification, and cofermentation operations. Section 4 presents and discusses the results from both the sensitivity analysis and the parameter estimation from experimental data for each unit operation. Finally, the conclusions are summarized in section 5.

2. PARAMETER ESTIMATION PROBLEM

A parameter estimation problem involves proposing a mathematical model of the process under study which contains unknown parameters that need to be determined by fitting the predicted model outputs to a set of experimental data.

In the field of chemical and biochemical engineering, a wide range of processes are represented by models consisting of systems of differential and algebraic equations (DAEs) with the first ones describing the dynamic behavior of the process. The associated parameter estimation problem is formulated as a DAE constrained optimization problem with the following general form:

$$\min \psi = \sum_{e=1}^{NE} \sum_{j=1}^{J_e} \sum_{m=1}^{M_{je}} (\hat{z}_{ejm} - z_{ejm})^T \mathbf{W}^{-1} (\hat{z}_{ejm} - z_{ejm}) \tag{1a}$$

subject to

$$\frac{d\mathbf{z}}{dt} = \mathbf{f}(\mathbf{z}, \mathbf{y}, \mathbf{p}, t) \tag{1b}$$

$$\mathbf{g}(\mathbf{z}, \mathbf{y}, \mathbf{p}, t) = \mathbf{0} \tag{1c}$$

$$\mathbf{z}(t_0) = \mathbf{z}^0 \qquad t \in [t_0, t_f] \tag{1d}$$

$$\mathbf{z}^L \le \mathbf{z} \le \mathbf{z}^U \tag{1e}$$

$$\mathbf{p}^L \le \mathbf{p} \le \mathbf{p}^U \tag{1f}$$

where $\hat{z}_{ejm}$ and z_{ejm} are the measured variables and the corresponding calculated values, respectively, for differential state variable j at point data m in experiment e, $\mathbf{W}$ is a diagonal weighting or scaling matrix, $\mathbf{f}$ is the right-hand-side vector in the differential equations, $\mathbf{g}$ is the algebraic constraints vector, t is the time, $\mathbf{y}$ is the algebraic state variables, $\mathbf{p}$ is the time-independent parameter vector which is to be estimated, and $\mathbf{z}^0$ is the initial conditions vector for state variables $\mathbf{z}$. It is considered that a total number of NE experiments are carried out under different conditions, and that a number of J_e state variables are measured. For each measurement j in every experiment e, a number of M_{je} data points are collected along the experiment duration.

In this formulation, the objective function ψ to be minimized is defined as the sum of the squared residues between the observed values and those predicted by the model.

2.1. Methodology. *2.1.1. Sensitivity Analysis.* In the field of chemical and biochemical engineering, many of the associated parameter estimation problems have a large number of parameters that must be estimated. Also, the number of available experimental measurements is generally limited. Therefore, attempting to identify a large number of parameters can result in significant errors on parameter estimates.

To assess the influence of the parameters on the model behavior, we perform sensitivity analysis. This technique is used to investigate variations in the output of the model resulting from variations in the parameters allowing the identification of those ones that have the largest impact on model variables. Sensitivity functions $\mathbf{S}_{\mathbf{z},p_k}$ and $\mathbf{R}_{\mathbf{y},p_k}$ represent the changes in model state differential variables $\mathbf{z}$ and algebraic variables $\mathbf{y}$, respectively, with respect to slight variations in the model parameter p_k defined by the following derivatives.

$$\mathbf{S}_{\mathbf{z},p_k}(t) = \frac{\partial \mathbf{z}}{\partial p_k}(t) \qquad \forall\, k$$
$$\mathbf{R}_{\mathbf{g},p_k}(t) = \frac{\partial \mathbf{g}}{\partial p_k}(t) \qquad \forall\, k \tag{2}$$

By differentiating the DAE system (eqs 1a−1f) with respect to the decisions $\mathbf{p}$ and changing the order of differentiation, the following sensitivity dynamic equations are obtained.[23]

dx.doi.org/10.1021/ie302358e | Ind. Eng. Chem. Res. 2013, 52, 4146−4160

$$\frac{d\mathbf{S}_{z,p_k}}{dt} = \frac{\partial \mathbf{f}}{\partial \mathbf{z}}\mathbf{S}_{z,p_k}(t) + \frac{\partial \mathbf{f}}{\partial \mathbf{y}}\mathbf{R}_{y,p_k}(t) + \frac{\partial \mathbf{f}}{\partial p_k},$$
$$\mathbf{S}_{z,p_k}(t_0) = \frac{\partial \mathbf{z}^0}{\partial p_k} \tag{3}$$
$$0 = \frac{\partial \mathbf{g}}{\partial \mathbf{z}}\mathbf{S}_{z,p_k}(t) + \frac{\partial \mathbf{g}}{\partial \mathbf{y}}\mathbf{R}_{y,p_k}(t) + \frac{\partial \mathbf{g}}{\partial p_k}$$

The solution of eqs 3 requires the state variables profiles resulting from the integration of the dynamic model (eqs 1a−1f). Therefore, in order to compute the sensitivities $\mathbf{S}_{p_k}$ and $\mathbf{R}_{p_k}$, eqs 3 have to be simultaneously solved with the dynamic system (eqs 1a−1f). The system is said to be sensitive to a certain parameter if a change in the parameter's value significantly affects the predictive quality of the model.[20] Thus, model parameters resulting in large values for the sensitivities have to be accurately estimated, while those ones whose sensitivity values are small are considered to be noninfluential parameters.[24]

2.1.2. Solution Strategy for Parameter Estimation Problem. A number of approaches, ranging from sequential methods to multiple shooting, to simultaneous collocation approaches,[25] have been used to solve the parameter estimation problem of eqs 1a−1f. Within the last approach, by using the method of orthogonal collocation over finite elements, the profiles of the state variables are fully discretized with respect to time, converting the dynamic system into a set of algebraic equations which are included directly in the formulation. As a result, the original DAE constrained optimization problem is transformed into a large-scale nonlinear programming (NLP) model.

In orthogonal collocation on finite elements, the time domain is divided into a number of elements NF and the state profiles in each finite element f are approximated by piecewise Lagrange polynomials of order NC + 1:

$$z_f^{NC+1}(t) = \sum_{q=0}^{NC} z_{fq}\varphi_q(t) \qquad \forall f \tag{4}$$

$$\varphi_q(t) = \prod_{q'=0,q'\neq q}^{NC} \frac{t - t_{fq'}}{t_{fq} - t_{fq'}} = \prod_{q'=0,q'\neq q}^{NC} \frac{\tau - \tau_{q'}}{\tau_q - \tau_{q'}} \qquad \forall q \tag{5}$$

where NC is the number of collocation points, $f \in \{1, ..., NF\}$ is a finite time element, $q \in \{1, ..., NC\}$ is a collocation point, $z_f^{NC+1}(t)$ is the (NC + 1)th order Lagrange polynomial at element finite f, and φ_q is a polynomial of degree NC. An important feature of Lagrange polynomials is that, at time point t_{fq}, the coefficient of the polynomial z_{fq} is the value of the state profile at that point. Then, these coefficients are treated as decision variables in the exact solution for the system at collocation points within each time element.[26] Note that the time variable, t, is normalized, τ, over each finite element such that $\tau \in [0, 1]$.

Thus, by using eqs 4 and 5, the DAEs are discretized forming residual equations at the time collocation points and forcing them to satisfy the model exactly. Furthermore, in order to ensure that the state variable profiles are continuous when crossing the time element boundaries, continuity constraints are imposed at the boundary collocation points.

In this way, the problem of eqs 1a−1f can be reformulated as an NLP problem as follows:

$$\min \psi = \sum_{e=1}^{NE}\sum_{j=1}^{J_e}\sum_{m=1}^{M_{je}} (\hat{z}_{ejm} - z_{ejm})^T \mathbf{W}^{-1}(\hat{z}_{ejm} - z_{ejm}) \tag{6a}$$

subject to

$$\sum_{q'=0}^{NC} z_{fq'je}\dot{\varphi}_{q'}(\tau_q) - \Delta h_f \mathbf{f}(z_{fqje}, \mathbf{p}, t_{fq}) = 0 \qquad \forall f, q, j, e \tag{6b}$$

$$\mathbf{g}(z_{fqje}, \mathbf{p}, t_{fq}) = \mathbf{0} \qquad \forall f, q, j, e \tag{6c}$$

$$z_{f,0,j,e} - \sum_{q=0}^{NC} z_{f-1,q,j,e}\varphi_q(\tau = 1) = 0 \qquad \forall j, e,$$
$$2 \le f \le NF \tag{6d}$$

$$z_{1,0,j,e} - z_{j,e}^0 = 0 \qquad \forall j, e \tag{6e}$$

$$z_{fqje}^L \le z_{fqje} \le z_{fqje}^U \qquad \forall f, q, j, e \tag{6f}$$

$$\mathbf{p}^L \le \mathbf{p} \le \mathbf{p}^U \tag{6g}$$

where $\dot{\varphi}_q = d\varphi/d\tau$, Δh_f is the length of finite element f, and τ_q is the normalized root of the Legendre polynomial of degree NC. Note that $\Delta h_f = h_{f+1} - h_f$, with h_f being the starting time of finite element f, and $t_{fq} = h_f + \Delta h_f \tau_q$.

In summary, within the simultaneous approach, the solution of the DAE system is directly coupled with the optimization problem and, thus, the DAE system is solved only once at the optimum point, avoiding intermediate solution steps that may not exist or may require excessive computational effort.[27]

3. UNIT OPERATION DESCRIPTIONS AND MATHEMATICAL MODELING

3.1. Dilute Acid Hydrolysis. Dilute acid hydrolysis has been used mainly as pretreatment for solubilizing the hemicellulosic fraction of lignocelluloses. Typically, it requires high temperatures (110−230 °C)[5−7,21] and pressures (~10 atm)[7] with acid concentrations below 5% w/w.[11] Sulfuric acid is the most widely used catalyst, although other acids, such as nitric and hydrochloric acids, have been also reported.[28,29] This operation makes the cellulose fraction more amenable for a subsequent enzymatic conversion, leaving the lignin fraction almost unaltered.

Reported studies are based mainly on agricultural and hardwood residues where xylan comprises the most relevant hemicelluloses.[30] In this work, xylan is considered as a heteropolymer containing xylose, arabinose, glucuronic acid, and acetyl groups substituting some hydroxyl groups of sugars.

Several kinetic approaches for describing the reaction rates of acid catalyzed hemicellulose hydrolysis have been proposed in the literature.[12,28,31−33] Most of them follow the model proposed by Saeman,[34] originally derived for cellulose hydrolysis, which assumes pseudohomogeneous first-order irreversible reactions in series.

In this work, we propose a model based on that of Lavarack et al.[12] for developing the parameter estimation problem of the hydrolysis step, catalyzed by dilute mineral acids. Several kinetic models of the overall rate of product formation for lignocellulosic biomass (e.g., sugarcane bagasse) have been proposed. In almost all schemes, the reaction rate has been assumed to be first order with respect to the reactants in each step. Furthermore, the kinetic rate constant for reaction step

dx.doi.org/10.1021/ie302358e | Ind. Eng. Chem. Res. 2013, 52, 4146−4160

i, k_i, varies with temperature following a modified Arrhenius relationship, where a power law dependence on the acid concentration is included.

Figure 1 shows the hydrolysis reactions considered in the present work. The formation of xylose (Xy), arabinose (Ara),

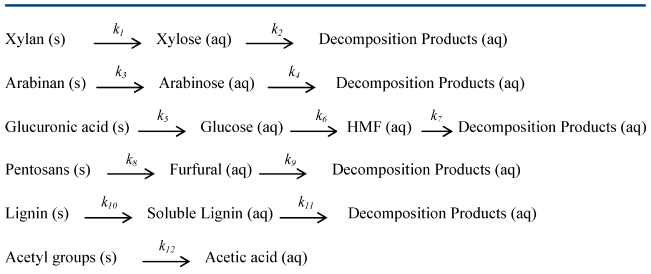

Figure 1. Reaction mechanisms for dilute acid hydrolysis.

glucose (G), and soluble lignin (SL) products follow the simplest scheme in Lavarack et al.[12] Under the aforementioned conditions used in the dilute acid hydrolysis operation, no glucose is considered to be released from the cellulose fraction of the lignocellulosic material. Nevertheless, small amounts of glucose are found in the hydrolysate which are assumed to be obtained from the glucuronic acid (GA) bound as lateral chains of the native xylan (Xn). As is well established, xylose and arabinose are further degraded to furfural (F) under acidic conditions. However, it is proposed that furfural is obtained only by the hydrolysis of pentosans, i.e., xylan (Xn) and arabinan (An) compounds, because the degradation of xylose is much slower than the reaction producing furfural.

In this paper, we have extended the model by Lavarack et al.[12] by including the production of acetic acid (AcH) released from the acetyl groups (AcG) attached to the xylan backbone. Furthermore, the HMF production from glucose degradation is added in the third reaction which, in turn, can be converted into decomposition products in a subsequent reaction step.

By taking the reaction mechanisms into account (Figure 1), and considering a first-order dependency of the reaction rates with concentration, the individual mass balances for the reactive species in the system are described by eqs 7 − 19.

$$\frac{dC_{Xn}}{dt} = -k_1 C_{Xn}\phi\rho \tag{7}$$

$$\frac{dC_{Xy}}{dt} = k_1 C_{Xn}\phi\rho - k_2 C_{Xy} \tag{8}$$

$$\frac{dC_{An}}{dt} = -k_3 C_{An}\phi\rho \tag{9}$$

$$\frac{dC_{Ara}}{dt} = k_3 C_{An}\phi\rho - k_4 C_{Ara} \tag{10}$$

$$\frac{dC_{GA}}{dt} = -k_5 C_{GA}\phi\rho \tag{11}$$

$$\frac{dC_{G}}{dt} = k_5 C_{GA}\phi\rho - k_6 C_{G} \tag{12}$$

$$\frac{dC_{HMF}}{dt} = k_6 C_{G} - k_7 C_{HMF} \tag{13}$$

$$\frac{dC_{F}}{dt} = k_8 (C_{Xn} + C_{An})\phi\rho - k_9 C_{F} \tag{14}$$

$$\frac{dC_{Ln}}{dt} = -k_{10} C_{Ln}\phi\rho \tag{15}$$

$$\frac{dC_{SL}}{dt} = k_{10} C_{Ln}\phi\rho - k_{11} C_{SL} \tag{16}$$

$$\frac{dC_{AcG}}{dt} = -k_{12} C_{AcG}\phi\rho \tag{17}$$

$$\frac{dC_{AcH}}{dt} = k_{12} C_{AcG}\phi\rho \tag{18}$$

$$k_i = k_i^0 C_{Ac}^{n_i} \exp\left(-\frac{E_i}{RT}\right) \qquad \forall\ i \tag{19}$$

where ϕ represents the solid material to liquid ratio used in the hydrolysis operation (kg kg^{-1}) and ρ is the density of the hydrolysate (kg L^{-1}). C_j represents the concentration of component j expressed in grams per kilogram for the species in the solid biomass (j = Xn, An, AcG, GA, Ln) and in grams per liter for the soluble products in the hydrolysate (j = Xy, Ara, G, F, HMF, AcH, SL).

Equation 19 represents the modified Arrhenius relationship for determining the reaction rate constant k_i of reaction step i, where k_i^0 is the pre-exponential or frequency factor (min^{-1}), C_{Ac} is the concentration of acid (wt %), n_i is the order of reaction with respect to C_{Ac}, E_i is the activation energy (J/mol), R is the universal gas constant (8.3144 J/mol K), and T is the temperature (K).

In summary, the parameter estimation problem in dilute acid hydrolysis leads to a DAE system with 12 differential equations (eqs 7−18) and 12 algebraic equations, one for each reaction step i, eq 19.

From this model, the set of kinetic parameters that should be estimated correspond to the frequency factors, k_i^0, exponents n_i, and activation energies E_i, for every reaction step i. The objective function eq 1a, defined as the sum of weighted squared errors between the observed species concentrations and the predicted values, is minimized, subject to model eqs 7−19 and the bound constraints on concentrations and parameters.

3.2. Detoxification. In the bioethanol process, a key problem associated with the dilute acid pretreatment is the unavoidable formation of byproducts that are harmful for the ensuing fermentation operation. The generation and concentration of microbial inhibitors are strongly influenced by temperature, reaction time, and acid concentration in the hydrolysis step.[35] Different types of inhibitory compounds are formed, which mainly correspond to three groups, i.e., furan derivatives (e.g., furfural and HMF), carboxylic acids (e.g., acetic, formic, and levulinic acids), and phenolic compounds.[11,13,36]

Accordingly, the efficiency of the subsequent ethanol fermentation is considerably decreased. Therefore, prior to this operation, a step for removing the toxicity of hydrolysates, the so-called detoxification step, has to be carried out. Several detoxification methods have been applied in the past, such as overliming, anion exchange, evaporation, and enzyme or microorganism treatment.[37] For a long time the calcium hydroxide overliming process has been considered the best one for dilute sulfuric acid pretreated hydrolysates.[13,38] This strategy is carried out by adding $Ca(OH)_2$ to the hydrolysate to raise the solution pH to 10−12, and maintaining this condition for a time period which ranges from 15 min to several days. Finally, the pH is adjusted to 5−7.[13,36,39] Nonetheless, this method presents drawbacks such as sugar degradation and gypsum ($CaSO_4$) precipitation when H_2SO_4 is used in pretreatment.

Despite the wide application of this detoxification technology, there is only one work (Purwadi et al.[13]), to our

dx.doi.org/10.1021/ie302358e | Ind. Eng. Chem. Res. 2013, 52, 4146−4160

knowledge, that presents a kinetic model for overliming. In our work, we extend this model to take into account process variables, such as pH and temperature.

As previously mentioned, furfural and HMF are formed by dehydration of sugars, pentoses and hexoses, respectively. On the basis of their relatively high concentration in lignocellulosic hydrolysates, several researchers[13,40,41] remarked that these furans are the dominant inhibitors to various fermentative microorganisms. Thus, the model includes not only these inhibitor degradations, but also sugar degradation. Figure 2 depicts the

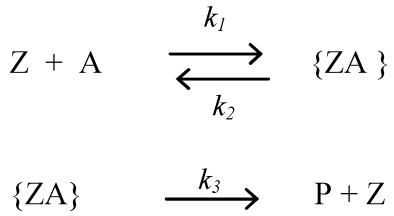

Figure 2. Reaction mechanisms for detoxification by overliming.

reaction mechanisms proposed. The process is described through two reactions, with the first one being reversible and exothermic. Here, each compound A (i.e., furfural, HMF, and sugars) reacts with cation Ca^{2+} denoted by Z, forming complex ions {ZA} which are, afterward, either converted to products P by the second reaction or to original species through the reverse reaction. Also, the amount of cation Ca^{2+} is limited by the quantity of anion OH^- which determines the pH level.

A simplified dynamic model of this operation is given by

$$\frac{dC_j}{dt} = -k_{1j}C_jC_Z + k_{2j}C_{Zj} \qquad \forall\, j \tag{20}$$

$$\frac{dC_{Zj}}{dt} = -(k_{2j} + k_{3j})C_{Zj} + k_{1j}C_jC_Z \qquad \forall\, j \tag{21}$$

$$\frac{dC_{Pj}}{dt} = k_{3j}C_{Zj} \qquad \forall\, j \tag{22}$$

$$\frac{dC_Z}{dt} = \sum_j (k_{2j} + k_{3j})C_{Zj} - k_{1j}C_jC_Z \tag{23}$$

where C_j represents the concentration of each reactant (j = F, HMF, S), C_Z is ion Ca^{2+} concentration, C_{Zj} is the concentration of transient complexes formed between each component j and calcium ions, and C_{Pj} is the product concentration of substance j, all expressed in grams per liter.

In this work, the reaction rate constants for every reaction step i, k_{ij}, in the kinetic model are assumed to follow an Arrhenius relationship described by an activation energy and a pre-exponential factor (eq 24).

$$k_{ij} = k_{ij}^0 \exp\left(-\frac{E_{ij}}{RT}\right) \qquad i = 1, 2, 3; \quad j = \text{F, HMF, S} \tag{24}$$

Moreover, to obtain the initial quantity of cation Z, C_Z^0, necessary for overliming, the following constraint is included.

$$C_Z^0 = k_z 10^{-c_1(14-\text{pH})} + c_2 \tag{25}$$

where k_z (g L^{-1}), c_1, and c_2 (g L^{-1}) are kinetic parameters. In eq 25 it can be seen that the initial concentration of $Ca(OH)_2$ is related to the pH level. Finally, the temperature dependence of the kinetic parameter k_z is modeled using the Arrhenius relationship in eq 26.

$$k_z = k_z^0 \exp\left(-\frac{E_z}{RT}\right) \tag{26}$$

where k_z^0 is the pre-exponential factor (g L^{-1}).

In summary, the DAE constrained optimization model for estimating kinetic parameters in the detoxification by overliming involves minimizing the sum of weighted squared errors (eq 1a) subject to 10 differential equations (eqs 20−23), 10 algebraic equations corresponding to the kinetic reaction constant for each reaction step (eq 24), and the expression defining the initial concentration for the cation (eq 25).

Therefore, kinetic parameters in this process are the frequency factors, k_{ij}^0 and k_z^0, the activation energies, E_i and E_z, and the parameters c_1 and c_2 in eq 25.

3.3. Cofermentation of Pentoses and Hexoses. The production of ethanol via the biochemical pathway involves the conversion of lignocellulosic feedstocks through saccharification and fermentation. The saccharification step involves the enzymatic hydrolysis of cellulose to glucose. Prior to this step, the aforementioned dilute acid pretreatment is necessary to make cellulose amenable to hydrolysis by cellulases. In order to be economically competitive, the resulting xylose-rich hydrolysate from the pretreatment step can be combined with the glucose produced from cellulose hydrolysis and both sugars can be simultaneously fermented to ethanol.

Saccharomyces cerevisiae and *Zymomonas mobilis*, the most frequently used microorganisms for bioethanol production, are not, however, able to ferment pentoses. *Z. mobilis* is an ethanologenic bacterium, generally considered as an economical high-performance biocatalyst for ethanol production at high rates compared to yeast.[42] Genetic engineering techniques have been applied for the synthesis of different recombinant strains of *Z. mobilis* capable of metabolizing both pentose and hexose sugars with high ethanol yields.[43] However, both sugar metabolization and ethanol production in these organisms can be inhibited by toxic compounds generated during the acid hydrolysis of lignocellulose.[39,44] Moreover, previous studies have shown that inhibitors can be converted in situ by fermenting organisms to less inhibitory compounds resulting in a long lag phase and a decrease in the potential production of ethanol. This behavior leads to significant changes over time in cell, substrate, and ethanol concentrations.

Although various unstructured kinetic models for cofermentation have been presented in the literature,[14,45,46] to our knowledge no previous attempts for including a description of the transformation of xenobiotic compounds, such as furfural, or their inhibitory effect on microbial growth kinetics have been addressed.

For this reason, one of the goals of this work is to propose a kinetic model for the fermentation of mixtures of glucose and xylose by *Z. mobilis* including the kinetics of furfural conversion, as well as its inhibiting impact on growth kinetics. We have extended the kinetic model proposed by Leksawasdi et al.,[14] which considers the simultaneous fermentation of xylose and glucose to ethanol by recombinant *Z. mobilis* strain ZM4-(pZB5). The unstructured mathematical model presented by those researchers includes substrate inhibition and product inhibition, as well as substrate limitation effects.

dx.doi.org/10.1021/ie302358e | Ind. Eng. Chem. Res. 2013, 52, 4146−4160

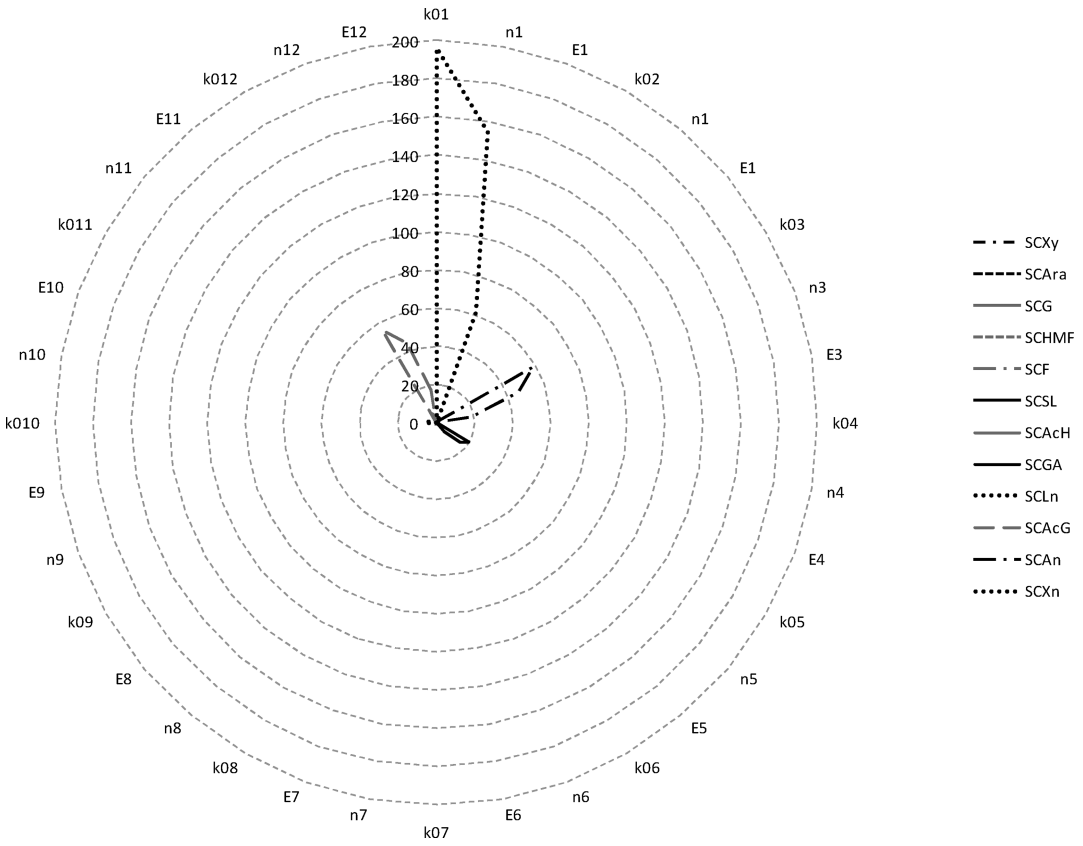

Figure 3. Maximum or minimum numerical absolute values of sensitivity profiles for the dilute acid hydrolysis model.

We have introduced a new term, which takes into account the inhibitory effect of furfural, not only on growth rate, but also on substrate consumption and product formation rates. In addition, in order to describe the conversion of furfural by the microorganism, a second-order kinetic has been adopted.

To formulate the double substrate model, Leksawasdi et al.[14] proposed that microbial growth on each sugar is represented by the specific growth rates of recombinant *Z. mobilis* on glucose and xylose as sole carbon sources. They assumed Monod type kinetics for both substrate and product inhibition. Also, as growth occurs on both sugars, they introduced weighting factors for glucose and xylose uptake, forcing the sum of these factors to be unity. By adding the contribution from each sugar, differential equations describing the time evolution of biomass formation, consumption of both substrates, and ethanol production were developed.

We propose the extended mathematical dynamic model describing the cofermentation of xylose and glucose, as follows:

$$\frac{dC_x}{dt} = [\alpha r_{x,G} + (1-\alpha) r_{x,Xy}] C_x \tag{27}$$

$$r_{x,G} = \mu_{max,G}\left(\frac{C_G}{K_{s,G}+C_G}\right)\left(1-\frac{C_{Et}-P_{i,G}}{P_{m,G}-P_{i,G}}\right)\left(\frac{K_{i,G}}{K_{i,G}+C_G}\right)\left(1-\frac{C_F}{C_{F,crit}}\right)^{n_G} \tag{28}$$

$$r_{x,Xy} = \mu_{max,Xy}\left(\frac{C_{Xy}}{K_{s,Xy}+C_{Xy}}\right)\left(1-\frac{C_{Et}-P_{i,Xy}}{P_{m,Xy}-P_{i,Xy}}\right) \times \left(\frac{K_{i,Xy}}{K_{i,Xy}+C_{Xy}}\right)\left(1-\frac{C_F}{C_{F,crit}}\right)^{n_{Xy}} \tag{29}$$

$$\frac{dC_G}{dt} = -\alpha q_{s,max,G}\left(\frac{C_G}{K_{s,G}+C_G}\right)\left(1-\frac{C_{Et}-P_{i,G}}{P_{m,G}-P_{i,G}}\right) \times \left(\frac{K_{i,G}}{K_{i,G}+C_G}\right)\left(1-\frac{C_F}{C_{F,crit}}\right)^{n_G} \tag{30}$$

$$\frac{dC_{Xy}}{dt} = -(1-\alpha) q_{s,max,Xy}\left(\frac{C_{Xy}}{K_{s,Xy}+C_{Xy}}\right)\left(1-\frac{C_{Et}-P_{i,Xy}}{P_{m,Xy}-P_{i,Xy}}\right) \times \left(\frac{K_{i,Xy}}{K_{i,Xy}+C_{Xy}}\right)\left(1-\frac{C_F}{C_{F,crit}}\right)^{n_{Xy}} C_x \tag{31}$$

$$\frac{dC_{Et}}{dt} = [\alpha r_{Et,G} + (1-\alpha) r_{Et,Xy}] C_x \tag{32}$$

$$r_{Et,G} = q_{p,max,G}\left(\frac{C_G}{K_{s,G}+C_G}\right)\left(1-\frac{C_{Et}-P_{i,G}}{P_{m,G}-P_{i,G}}\right) \times \left(\frac{K_{i,G}}{K_{i,G}+C_G}\right)\left(1-\frac{C_F}{C_{F,crit}}\right)^{n_G} \tag{33}$$

$$r_{Et,Xy} = q_{p,max,Xy}\left(\frac{C_{Xy}}{K_{s,Xy}+C_{Xy}}\right)\left(1-\frac{C_{Et}-P_{i,Xy}}{P_{m,Xy}-P_{i,Xy}}\right) \times \left(\frac{K_{i,Xy}}{K_{i,Xy}+C_{Xy}}\right)\left(1-\frac{C_F}{C_{F,crit}}\right)^{n_{Xy}} \tag{34}$$

$$\frac{dC_F}{dt} = -k_f C_F C_x \tag{35}$$

dx.doi.org/10.1021/ie302358e | *Ind. Eng. Chem. Res.* 2013, 52, 4146−4160

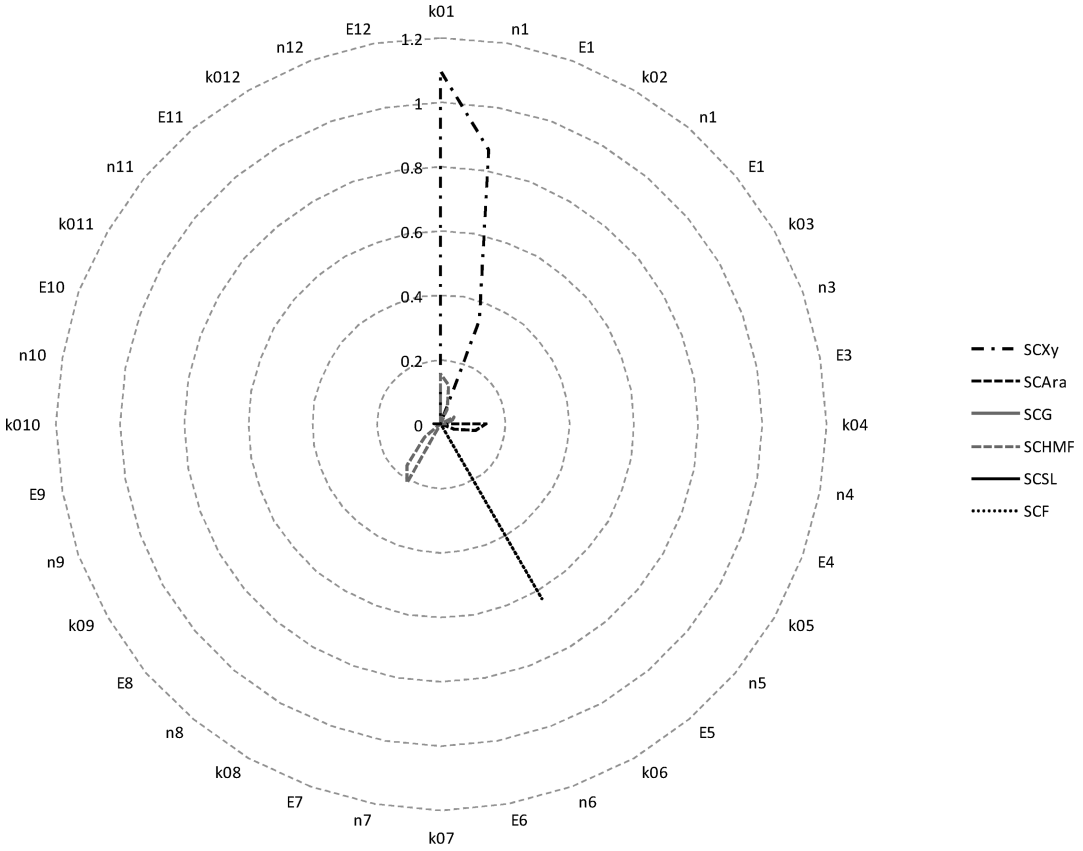

Figure 4. Maximum or minimum numerical absolute values of sensitivity profiles for state variables in dilute acid hydrolysis model (low numerical values).

where α is the weighting factor for glucose consumption, $r_{x,G}$ and $r_{x,Xy}$ are the rates of biomass production, and $r_{Et,G}$ and $r_{Et,Xy}$ are the ethanol production rates from glucose and xylose, respectively.

In the above equations, C_{Xy} (g L^{-1}) represents the xylose concentration, C_G (g L^{-1}) is the glucose concentration, C_{Et} (g L^{-1}) is the ethanol concentration, C_x (g L^{-1}) is the cell mass concentration, and C_F (g L^{-1}) is the furfural concentration. Parameters $K_{s,G}$ and $K_{s,Xy}$ are the saturation constants, while $\mu_{max,G}$ and $\mu_{max,Xy}$ are the maximum specific growth rates of the microorganism in glucose and xylose fermentations, respectively. $q_{s,max,G}$ and $q_{s,max,Xy}$ are maximum specific uptake rates, while $q_{p,max,G}$ and $q_{p,max,Xy}$ are ethanol production rates in glucose and xylose fermentations, respectively. $K_{i,G}$ and $K_{i,Xy}$ account for the substrate inhibition in glucose and xylose fermentation, respectively. $P_{m,G}$ and $P_{m,Xy}$ are the maximum concentrations of ethanol above which cells do not produce ethanol, while $P_{i,G}$ and $P_{i,Xy}$ are the threshold ethanol concentrations from glucose and xylose fermentations. We introduced parameters $C_{F,crit}$, n_G, and n_{Xy} to account for the fact that the presence of furfural in the fermentation media produces an inhibitory effect on cell growth and ethanol production. $C_{F,crit}$ (g L^{-1}) denotes the critical concentration of furfural causing the complete inhibition of *Z. mobilis* growth, while n_G and n_{Xy} are unitless inhibition factors for glucose and xylose, respectively. The value of the parameter $C_{F,crit}$ is 2.375 g L^{-1}, which has been determined from earlier works published in the literature.[11,22,44]

It should be noted that, in ethanol production from two substrates, both biomass and ethanol production rates in eqs 27 and 32 are expressed through the weighted sum of the corresponding production rates on sole substrates, glucose and xylose, respectively. Furthermore, the original set with a large number of estimated parameters by Leksawasdi et al.[14] is significantly reduced in our study.

We have considered furfural consumption by the fermenting microorganism as a second-order rate expression that depends

Table 1. Working Conditions for Dilute Acid Hydrolysis[21]

expt	temp (°C)	H_2SO_4 (wt %)
1	135	1.5
2	118	1.7
3	153	1.7
4	110	2.2
5	135	2.2
6	160	2.2
7	118	2.7
8	153	2.7
9	135	3.0

Table 2. Parameter Values Determined by Fitting the Hydrolysis Model

parameter	optimal value	parameter	optimal value
k_1^0	4.091×10^9	E_5	45.670
n_1	1.391	k_{10}^0	1.025×10^3
E_1	76.361	n_{10}	0.100
k_3^0	8.454×10^4	E_{10}	15.240
n_3	0.984	k_{12}^0	1.857×10^{17}
E_3	35.092	n_{12}	0.095
k_5^0	1.860×10^6	E_{12}	144.055
n_5	0.616		

dx.doi.org/10.1021/ie302358e | *Ind. Eng. Chem. Res.* 2013, 52, 4146−4160

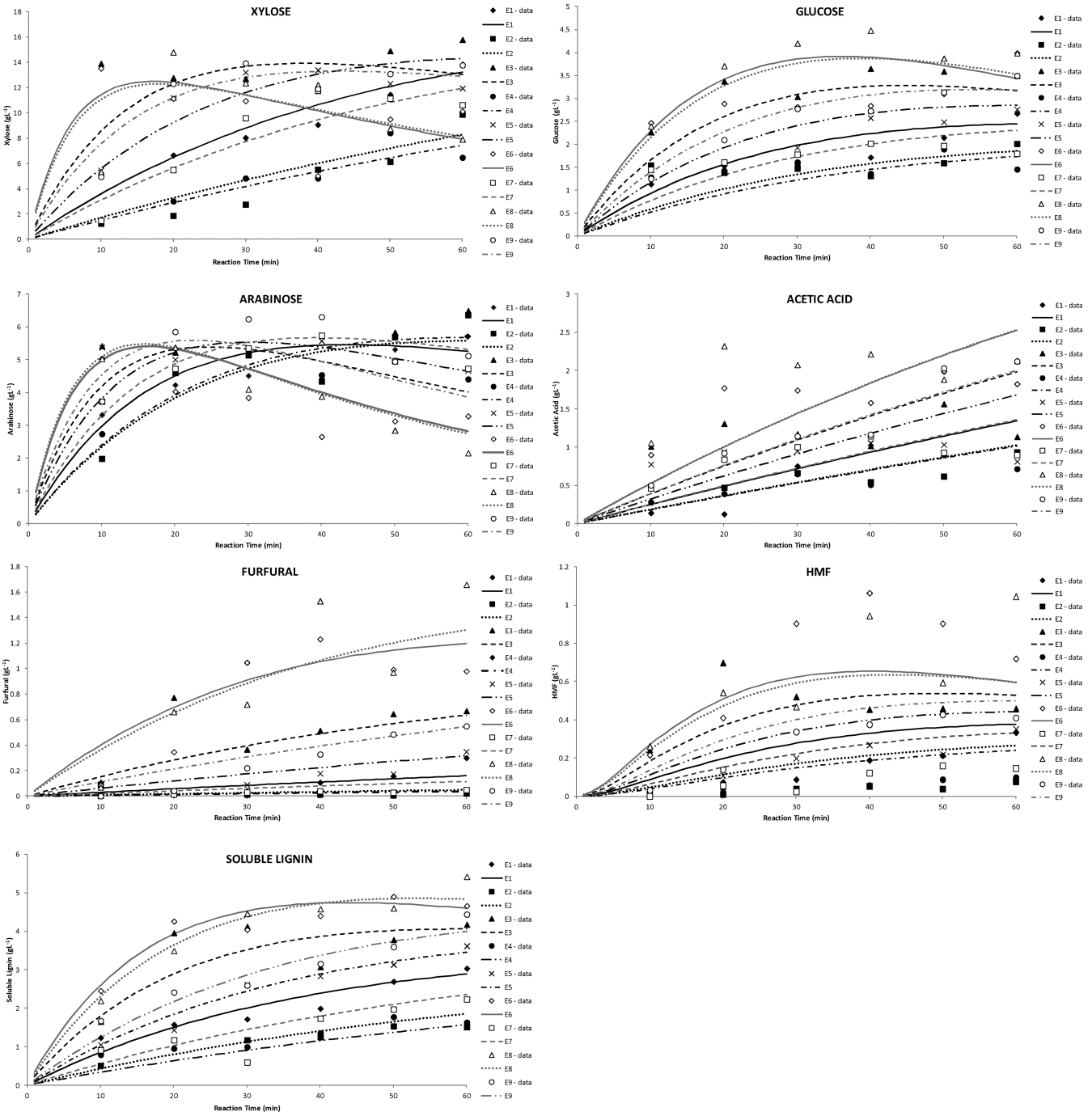

Figure 5. Concentration profiles for xylose, glucose, arabinose, furfural, HMF, and soluble lignin in dilute acid hydrolysis carried out at different conditions: (experiment 1) 408 K, 1.5% H_2SO_4; (experiment 2) 391 K, 1.7% H_2SO_4; (experiment 3) 426 K, 1.7% H_2SO_4; (experiment 4) 383 K, 2.2% H_2SO_4; (experiment 5) 408 K, 2.2%; (experiment 6) 433 K, 2.2% H_2SO_4; (experiment 7) 391 K, 2.7% H_2SO_4; (experiment 8) 426 K, 2.7% H_2SO_4; (experiment 9) 408 K, 3.0% H_2SO_4. The symbols are experimental data points, and continuous lines represent model predictions.

Table 3. Average Deviations between Measured and Predicted Values for Main Components in the Hydrolysis Model

average deviation						
xylose	arabinose	glucose	furfural	HMF	AcH	SL
−0.0259	0.0449	0.0614	−0.0189	−0.0467	0.0815	0.0288

on the concentrations of furfural and active biomass. This expression better represents experimental data from the literature.

In summary, the problem of estimating kinetic parameters in cofermentation consists of minimizing the weighted least squared objective function, ψ (eq 1a) subject to five differential equations, eqs 27, 30−32, and 35, and bound constraints on concentration values and parameters. Here, model parameters correspond to maximum specific growth rates, maximum specific uptake rates, inhibition constants, maximum concentration

dx.doi.org/10.1021/ie302358e | Ind. Eng. Chem. Res. 2013, 52, 4146−4160

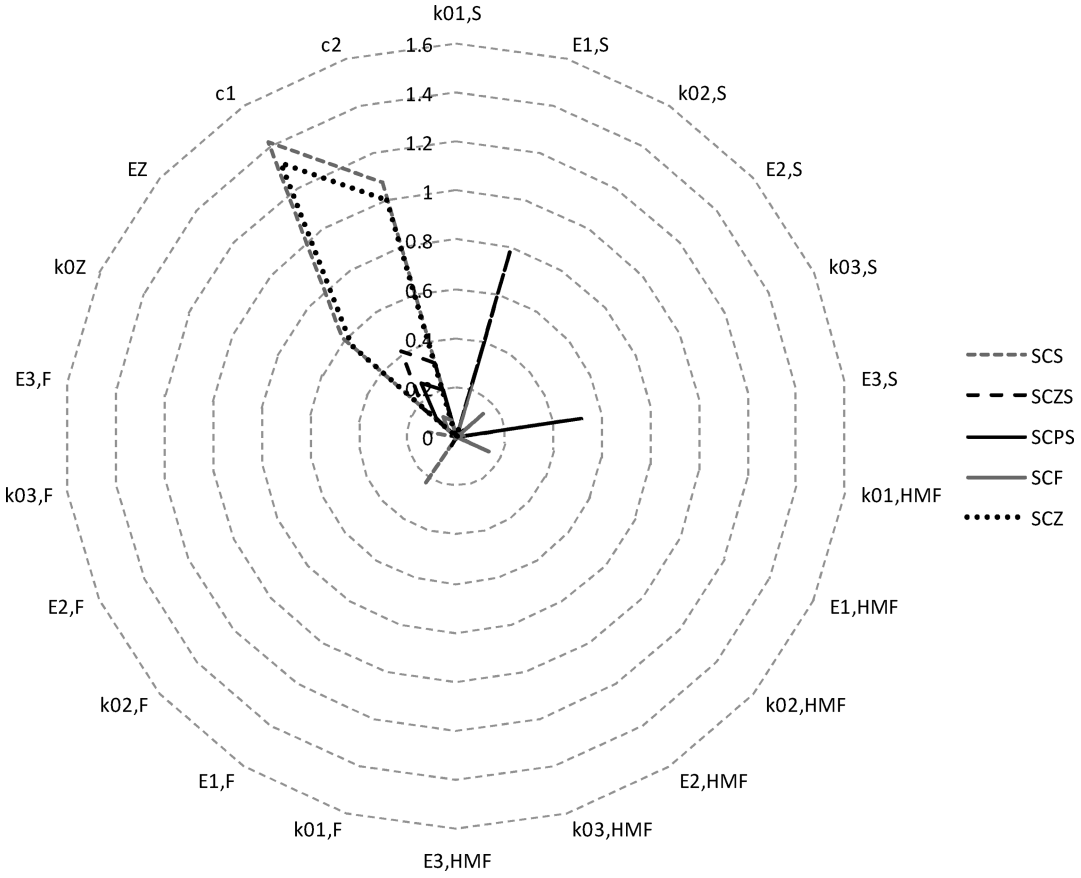

Figure 6. Maximum or minimum numerical absolute values of sensitivity profiles for C_S, C_{ZS}, C_F, C_{PS}, and C_Z in the detoxification model.

of product, threshold ethanol concentration, and inhibition factors for glucose and xylose fermentations.

4. NUMERICAL RESULTS AND DISCUSSION

As a first step, we perform sensitivity analysis on the parameters in each process operation described in section 3 to identify those that have to be estimated. Parameter sensitivity calculations have been developed with Matlab 7.6.0 (The MathWorks, Inc.). Hereafter, parameter estimation with a reduced number of parameters for dilute acid hydrolysis, detoxification, and cofermentation models is carried out, using experimental data from the literature. All models have been implemented in the GAMS modeling environment,[19] and they have been solved using full space SQP techniques within an interior point algorithm with the IPOPT solver.[18] In order to test the quality of the proposed models, graphical comparison of the measured values with the predicted outputs will be included.

4.1. Acid Hydrolysis Model Fit. The state vector, **z**, is composed of concentrations C_j and the parameter vector, **p**, is made up of k_i^0, n_i, and E_i, for 12 reaction steps presented in Figure 1, resulting in 36 total parameters. Given the large number of parameters to be identified, a sensitivity study from model variables toward these parameters is performed to reduce the number of parameters, allowing their identification with available experimental data. We evaluate sensitivity functions $\mathbf{S}_{z,p_k}$ for a given parameter set showing the sensitivity of each output C_j respect to small variations on the above-mentioned parameters. The resulting trajectories of the sensitivity functions can be plotted for each model output with respect to each parameter variation. For the sake of clarity, instead of presenting each sensitivity trajectory, Figure 3 shows the maximum and minimum values of each sensitivity function, in absolute values. This figure allows detecting the parameters which are the most influential ones on each model state variable. The maximum values are obtained for parameters k_1^0, n_1, E_1, k_3^0, n_3, E_3, k_5^0, n_5, E_5, k_{10}^0, n_{10}, E_{10}, k_{12}^0, n_{12}, and E_{12}, which can be seen from Figure 3 except for k_{10}^0, n_{10}, and E_{10}. In the Appendix, Table 8 shows the remaining model parameters and their values. Also, Figure 4 is included in order to show the modulus of the maximum or minimum values of the sensitivity functions of the state variables whose order of magnitude is much lower than those shown in Figure 3. In this way, the number of parameters has been reduced to 15, considering those for which the absolute value of the maximum sensitivity function is greater than 1.0.

Parameter estimation in the dilute acid hydrolysis model has been performed based on experimental data from Cassales et al.[21] These authors carried out several assays aiming at obtaining the optimal conditions for the dilute acid hydrolysis of soybean hull to achieve maximal sugar yields (xylose, arabinose, and glucose) while minimizing the liberation of microbial inhibitory compounds. A total number of nine experiments (NE = 9) under different temperatures and sulfuric acid concentrations were performed over 60 min reaction time, taking samples in time intervals of 10 min. The values of temperatures and acid concentrations employed in each experiment are given in Table 1. Moreover, the solid biomass to liquid ratio, ϕ, is fixed at 0.10 g g^{-1} in all the experiments.

The parameter estimation problem for the dilute acid hydrolysis has 108 differential equations for the nine experiments

dx.doi.org/10.1021/ie302358e | Ind. Eng. Chem. Res. 2013, 52, 4146−4160

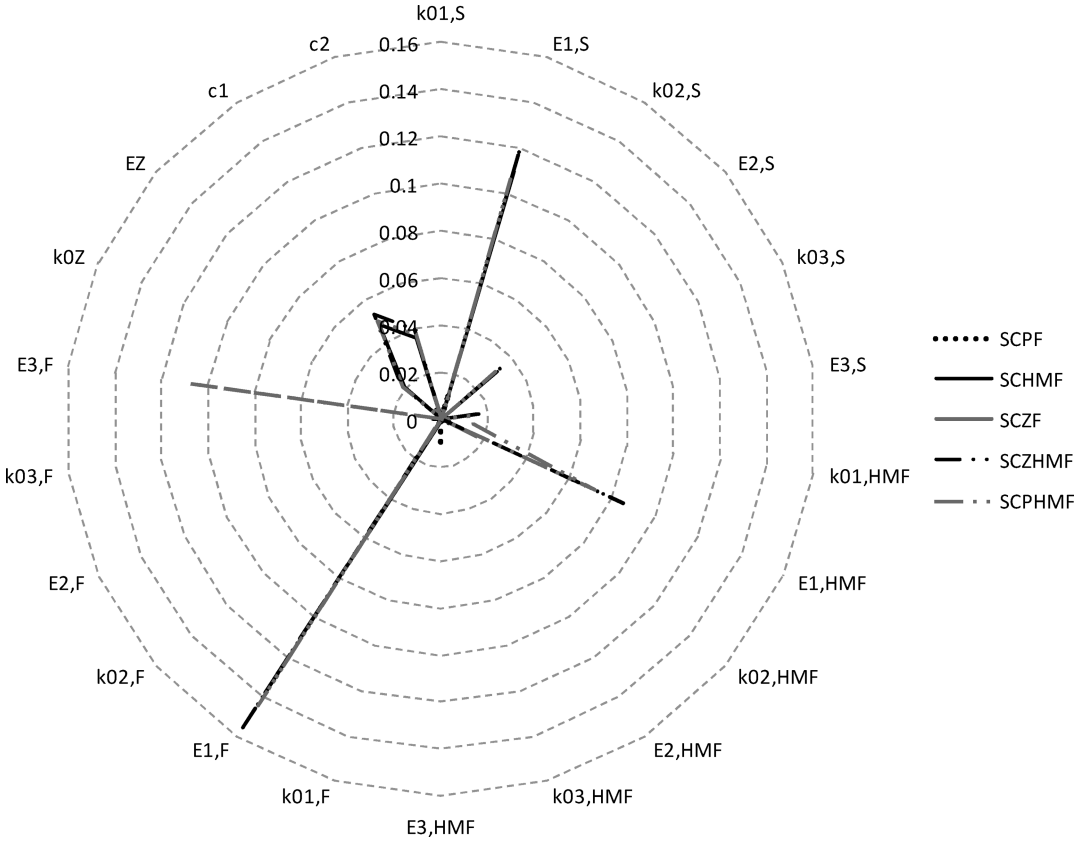

Figure 7. Maximum or minimum numerical absolute values of sensitivity profiles for C_{HMF}, C_{ZHMF}, C_{PHMF}, C_F, C_{ZF}, and C_{PF} in the detoxification model.

and six points for each state variable per experiment (M_{je} = 6). The initial conditions for each experiment e, $\mathbf{z}^0$, are the mass compositions of each component in the soybean hull on a dry basis.[21]

The DAE constrained optimization problem, described in section 3.1, is transformed into an NLP one by considering a time discretization with five finite elements and using fourth-order Lagrange polynomials. The resulting NLP formulation comprises 2584 equations and 2599 variables which consist of 15 parameters and 2584 collocation coefficients.

The parameters obtained from fitting the experimental data to the model outcomes are presented in Table 2. Figure 5 shows the xylose, glucose, arabinose, acetic acid, furfural, HMF, and soluble lignin profiles compared to the measured concentrations of these products during the hydrolysis process. Moreover, the model performance for calibration has been assessed quantitatively by the average deviations for the main state variables of the model. The average values of the deviations between the model predictions and the observed data for concentrations in the hydrolysis model are summarized in Table 3. An inspection of Figure 5 and Table 3 reveals a good agreement between model predictions and measurements with the highest mean deviation being equal to 8.1%.

4.2. Detoxification Model Fit. In the detoxification model, the state vector, $\mathbf{z}$, comprises concentrations C_j, C_Z, C_{Zj}, and C_{Pj}; the parameter vector, $\mathbf{p}$, is composed of k_{ij}^0, k_z^0, E_{ij}, E_z, c_1, and c_2 comprising a total of 22 elements. Based on the analysis of the sensitivity functions $\mathbf{S}_{z,p_k}$ obtained through a sensitivity study for this operation, the most influential parameters that have to be estimated are nine, namely $E_{1,S}$, $E_{2,S}$, $E_{3,S}$, $E_{1,HMF}$, $E_{1,F}$, $E_{3,F}$, E_z, c_1, and c_2. Figures 6 and 7 show the maximum or minimum absolute values of the sensitivity trajectories for the detoxification model. Figure 6 shows the sensitivities for output variables C_S, C_{ZS}, C_F, C_{PS}, and C_Z, which present the larger variations to the parameters. In Figure 7 the sensitivities for state variables C_{HMF}, C_{ZHMF}, C_{PHMF}, C_F, C_{ZF}, and C_{PF} are shown where the aforementioned parameters have a lower influence.

Table 4. Parameter Values Determined by Fitting the Detoxification Model

parameter	optimal value	parameter	optimal value
$E_{1,S}$	22.414	$E_{1,HMF}$	33.510
$E_{2,S}$	66.822	E_z	14.622
$E_{3,S}$	63.079	c_1	0.460
$E_{1,F}$	16.532	c_2	1.000
$E_{3,F}$	62.501		

In this work, we have carried out parameter estimation for detoxification of hydrolysates by overliming. Experimental data have been obtained from Purwadi et al.[13] These authors performed a two-stage dilute acid hydrolysis of forest residues using H_2SO_4 as catalyst. In the first stage the hydrolysis of hemicelluloses takes place, while in the second one the cellulose fraction is hydrolyzed. For estimating the parameters of the detoxification model given in section 3.2, only the first-stage measurements are used in this work since the reaction conditions (temperature, pressure, and acid concentration) correspond to those of the dilute acid hydrolysis pretreatment in section 3.1.

Purwadi et al.[13] have carried out a total of 12 experiments (NE = 12) by adding calcium hydroxide to the hydrolysates up

dx.doi.org/10.1021/ie302358e | Ind. Eng. Chem. Res. 2013, 52, 4146−4160

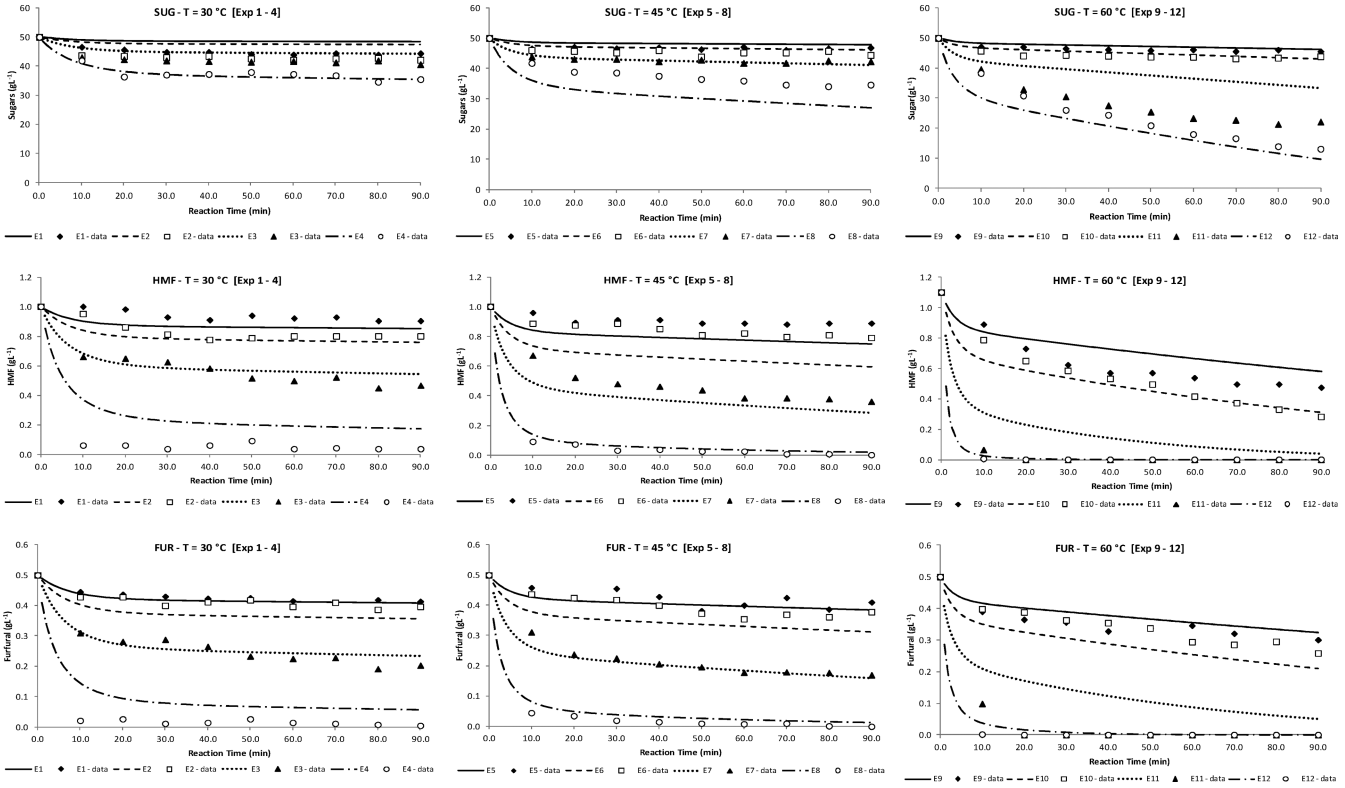

Figure 8. Concentration profiles for sugars, furfural, and HMF in detoxification carried out at different conditions: (experiment 1) 30 °C, pH 9; (experiment 2) 30 °C, pH 10; (experiment 3) 30 °C, pH 11; (experiment 4) 30 °C, pH 12; (experiment 5) 45 °C, pH 9; (experiment 6) 45 °C, pH 10; (experiment 7) 45 °C, pH 11; (experiment 8) 45 °C, pH 12; (experiment 9) 60 °C; pH 9; (experiment 10) 60 °C, pH 10; (experiment 11) 60 °C, pH 11; (experiment 12) 60 °C, pH 12. The symbols are experimental data points, and continuous lines represent predicted values.

Table 5. Average Deviations between Measured and Predicted Values for Main Components in the Detoxification Model

average deviation		
sugar	HMF	furfural
−1.1749	0.0059	−0.0026

Table 6. Parameter Values Determined by Fitting the Cofermentation Model

parameter	optimal value	parameter	optimal value
α	0.600	$P_{m,G}$	6.669
$\mu_{max,G}$	0.010	$P_{m,Xy}$	9.469
$\mu_{max,Xy}$	0.017	$P_{i,G}$	6.575
$K_{i,G}$	1.000	$P_{i,Xy}$	9.308

to four different pH levels (i.e., 9.0, 10.0, 11.0, and 12.0) at three temperatures (i.e., 30, 45, and 60 °C). The concentrations of furfural, HMF, and sugars were monitored every 10 min during a time horizon of 90 min (M_{je} = 9).

In this case, the initial concentrations, $\mathbf{z}^0$, are the same for all compounds j in each experiment except for the cation concentration, which is calculated by eq 25 as a function of the temperature and pH level.

After discretization of the DAE constrained problem proposed in section 3.3, the resulting NLP parameter estimation problem has 11233 algebraic equations and 11242 variables. State profiles are obtained solving the model with 18 equal-sized finite elements and three collocation points within each element.

Table 4 lists the obtained parameter values for detoxification, and Table 9 in the Appendix presents the remaining parameter values. Figure 8 shows a comparison between concentration profiles (continuous lines) predicted by the detoxification model and experimental data (symbols). It can be seen that the model is able to capture the observed behavior in a satisfactory way.

Table 5 shows average values of deviations for concentrations in the detoxification model.

4.3. Cofermentation Model Fit. Prior to parameter estimation, a sensitivity analysis on the cofermentation model is carried out, allowing the identification of the most influential parameters on the dynamics of this operation. Analyzing the trajectories of the sensitivity functions of the process α, $\mu_{max,G}$, $\mu_{max,Xy}$, $K_{i,G}$, $P_{m,G}$, $P_{m,Xy}$, $P_{i,G}$, and $P_{i,Xy}$ have been identified as the eight most influential parameters for all the state variables. From this analysis, 10 of the 18 analyzed parameters are not influential on state variables and they are considered to have constant known values (see Table 10 in the Appendix).

Figure 9 presents the maximum or minimum numerical values, in absolute value, for the sensitivity functions in the operation of cofermentation. In this way, the number of parameters has been reduced to eight, considering those for which the absolute value of the maximum sensitivity function is greater than 1.0.

In parameter estimation for the cofermentation model, we use experimental data from Gutierrez-Padilla and Karim.[22] These authors carried out an experimental study to evaluate the inhibitory effect of furfural on the recombinant *Z. mobilis* strain CP4(pZB5) in the production of bioethanol. Three experiments (NE = 3) with different initial concentrations of furfural

dx.doi.org/10.1021/ie302358e | Ind. Eng. Chem. Res. 2013, 52, 4146−4160

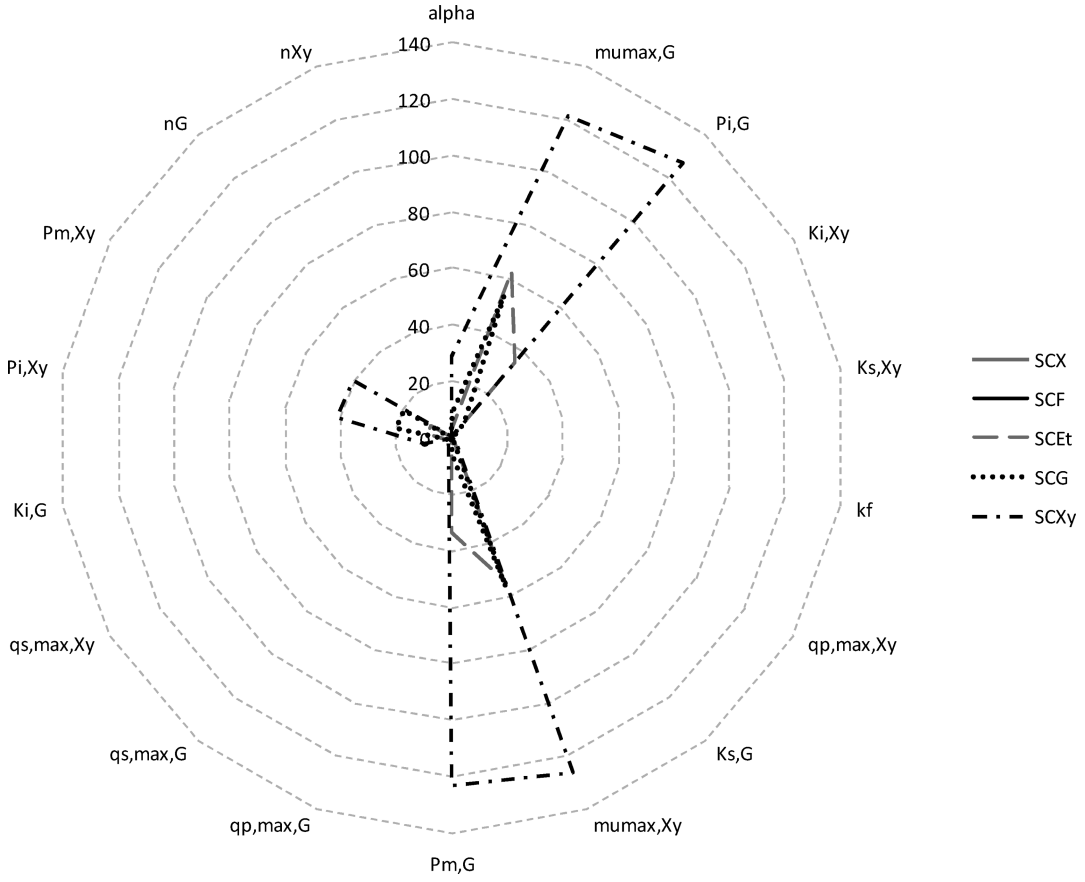

Figure 9. Maximum or minimum numerical absolute values of sensitivity profiles for the cofermentation model.

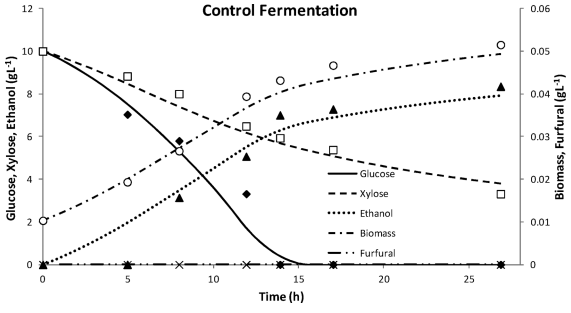

Figure 10. Observed data and simulation profiles in the fermentation carried out without furfural: (experiment 1) 0 g L^{-1}. Experimental data points for (◆) glucose, (□) xylose, (▲) ethanol, (○) biomass and (×) furfural concentrations. Continuous lines represent model predictions.

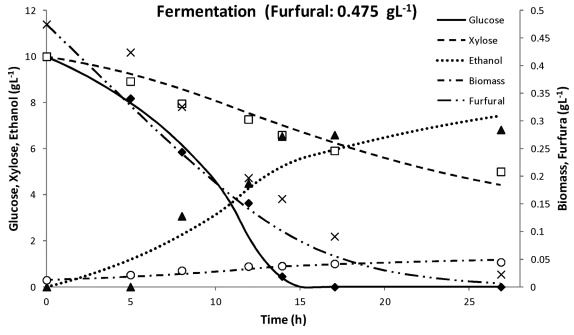

Figure 11. Observed data and simulation profiles in the fermentation carried out with 0.475 g of furfural L^{-1}: (experiment 2) 0.475 g L^{-1}. Experimental data points for (◆) glucose, (□) xylose, (▲) ethanol, (○) biomass, and (×) furfural concentrations. Continuous lines represent model predictions.

in the fermentation media were reported. Specifically, two fermentations by adding furfural 10 h after inoculation between lag and exponential phases achieving initial furfural concentrations of 0.475 and 1.9 g L^{-1} and control fermentations with no furfural supply have been also carried out. The concentrations of biomass (C_x), furfural (C_F), glucose (C_G), xylose (C_{Xy}), and ethanol (C_{Et}) have been measured at several time intervals over a 40 h range in each experiment.

In the cofermentation model presented in section 3.3, the aforementioned concentrations are the state variables (vector **z**). Parameter vector **p** is originally composed of 18 parameters corresponding to maximum specific rates (growth, uptake, and production), inhibition constants, and inhibition factors. It should be noted that only the initial concentration of furfural is different in each experiment *e*. Experimental data are fitted using third-order Lagrange polynomials on five finite elements. After performing the sensitivity analysis, the aforementioned eight model parameters were estimated using the three sets of experimental data simultaneously. For the optimization procedure, the initial values of the parameters to be estimated were taken from the literature.[14]

Estimated parameters are summarized in Table 6. Figures 10−12 depict the observed concentration values for each compound (points) vs main state variable profiles (solid lines) in every experiment. Additionally, in order to get a better visualization, simulation results of biomass growth in each experiment are presented in Figure 13. It is important to note that the simulated

dx.doi.org/10.1021/ie302358e | Ind. Eng. Chem. Res. 2013, 52, 4146−4160

Table 7. Average Deviations between Measured and Predicted Values and for Main Components in the Cofermentation Model

average deviation				
biomass	glucose	xylose	ethanol	furfural
0.0026	−0.2268	−0.2229	0.1631	−0.1358

Table 8. Model Parameters for the Dilute Acid Hydrolysis Model

parameter	value	parameter	value
k_1^0	estimated	k_7^0	1.33×10^4
n_1	estimated	n_7	0.680
E_1	estimated	E_7	30.007
k_2^0	6.85×10^{10}	k_8^0	1.06×10^8
n_2	1.709	n_8	0.566
E_2	86.572	E_8	63.439
k_3^0	estimated	k_9^0	2.15×10^6
n_3	estimated	n_9	0.100
E_3	estimated	E_9	48.395
k_4^0	1.14×10^5	k_{10}^0	estimated
n_4	0.940	n_{10}	estimated
E_4	36.783	E_{10}	estimated
k_5^0	estimated	k_{11}^0	2.82×10^{11}
n_5	estimated	n_{11}	1.944
E_5	estimated	E_{11}	116.776
k_6^0	4.91×10^2	k_{12}^0	estimated
n_6	0.100	n_{12}	estimated
E_6	19.023	E_{12}	estimated

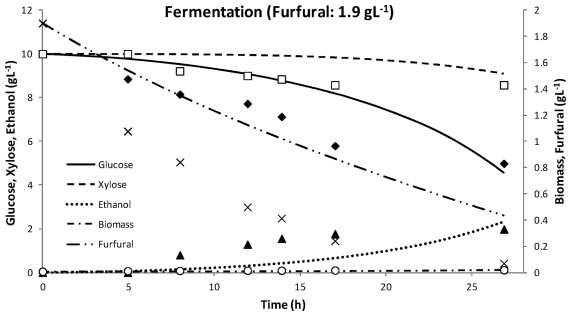

Figure 12. Observed data and simulation profiles in fermentation carried out with 1.9 g of furfural L^{-1}: (experiment 3) 1.9 g L^{-1}. Experimental data points for (◆) glucose, (□) xylose, (▲) ethanol, (○) biomass, and (×) furfural concentrations. Continuous lines represent model predictions.

Table 9. Model Parameters for the Detoxification Model

parameter	value	parameter	value
$k_{1,S}^0$	3352.280	$k_{3,F}^0$	2×10^9
$E_{1,S}$	estimated	$E_{3,F}$	estimated
$k_{2,S}^0$	2×10^9	$k_{1,HMF}^0$	2×10^5
$E_{2,S}$	estimated	$E_{1,HMF}$	estimated
$k_{3,S}^0$	2×10^9	$k_{2,HMF}^0$	10 482.168
$E_{3,S}$	estimated	$E_{2,HMF}$	94.491
$k_{1,F}^0$	1000.000	$k_{3,HMF}^0$	2×10^9
$E_{1,F}$	estimated	$E_{3,HMF}$	63.544
$k_{2,F}^0$	10795.295	k_z^0	2 225 559.198
$E_{2,F}$	129.752	E_z	estimated
c_1	estimated	c_2	estimated

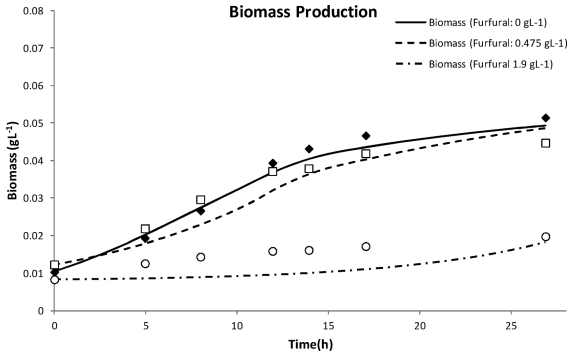

Figure 13. Observed data and simulation profiles for biomass concentration in fermentation carried out at different furfural concentrations: (experiment 1, ◆) 0, (experiment 2, □) 0.475, and (experiment 3, ○) 1.9 g L^{-1}. Symbols correspond to experimental data points, and continuous lines represent model predictions.

Table 10. Model Parameters for the Cofermentation Model

parameter	value	parameter	value
α	estimated	$P_{i,G}$	estimated
$\mu_{max,G}$	estimated	$P_{i,Xy}$	estimated
$\mu_{max,Xy}$	estimated	$P_{m,G}$	estimated
$K_{s,G}$	0.010	$P_{m,Xy}$	estimated
$K_{s,Xy}$	25.459	$q_{s,max,G}$	9.200
$K_{i,G}$	estimated	$q_{s,max,Xy}$	3.836
$K_{i,Xy}$	550.000	$q_{p,max,G}$	2.707
n_G	1.461	$q_{p,max,Xy}$	3.080
n_{Xy}	4.432	k_f	5.017

profiles and experimental data in Figures 10−13 are presented in the 30 h range because this is the time period where furfural is present in the fermentation media. As can be seen, the deviations between model predictions and experimental data occur mainly in the furfural concentration profile. Also, the average values of deviation for concentrations of main components in the cofermentation model are listed in Table 7.

It can be noted that the best fits are obtained for cofermentation without furfural, but there is still good agreement for increasing furfural concentrations. To our knowledge, this is the first model proposed for cofermentation in the presence of furfural. After appropriate scaling, the model can be used for process optimization and determination of the need of a detoxification step in the biochemical production of ethanol.

5. CONCLUSIONS

In this study, we propose new model formulations and kinetic parameter estimation in dilute acid hydrolysis, detoxification, and cofermentation, which are main process operations in the biochemical pathway for ethanol production.

Model parameter estimation is accomplished by minimizing a weighted least squares objective function subject to process constraints represented by a DAE system. These models are solved by using a simultaneous solution approach in which the DAEs are fully discretized in time. This procedure gives rise to large-size NLP optimization problems which are solved with an interior point (IP) method with sequential quadratic programming (SQP) strategies within the program IPOPT.

Prior to performing parameter estimation, the number of kinetic parameters has been reduced through a sensitivity analysis, which allows the identification of the most influential ones in each process model. The selection of the model

dx.doi.org/10.1021/ie302358e | Ind. Eng. Chem. Res. 2013, 52, 4146−4160

parameters that need to be estimated was based on a comparison of the maximum or minimum absolute values of the corresponding sensitivity trajectories.

Then, a reduced number of kinetic parameters have been estimated using different sets of previously reported experimental data.[13,21,22] Numerical results show a satisfactory adjustment between observed and simulated profiles, concluding that the proposed models for acid hydrolysis, detoxification, and cofermentation are able to describe the corresponding experimental data behavior.

The proposed model, with appropriate scale-up, will be used in optimization of ethanol production through the biochemical pathway. The inclusion of furfural influence on the cofermentation process, together with the detoxification model, enables structural optimization, determining whether the detoxification step is required within the process.

APPENDIX

Tables 8, 9, and 10 list the remaining model parameters for the dilute acid hydrolysis model, the detoxification model, and the cofermentation model, respectively.

AUTHOR INFORMATION

Corresponding Author

*Tel.: +54-0291-4861700. Fax: +54-0291-4861600. E-mail: smoreno@plapiqui.edu.ar.

Notes

The authors declare no competing financial interest.

ACKNOWLEDGMENTS

The authors would like to thank the Consejo Nacional de Investigaciones Científicas y Técnicas (CONICET), Agencia Nacional de Promoción Científica y Tecnológica (ANPCyT), and Universidad Nacional del Sur (UNS) from Argentina for financial support.

NOTATION

Subscripts

e = experiment
f = finite time element
m = data point
i = reaction step
j = product
k = parameter
q = collocation point

Superscripts

L = lower bound
U = upper bound
0 = initial value

Parameters

C_j = concentration of component j (g L^{-1})
C_{Ac} = sulfuric acid concentration in hydrolysis operation (wt %)
C_{AcG} = acetyl group concentration in lignocellulosic biomass (g kg^{-1})
C_{An} = arabinan concentration in lignocellulosic biomass (g kg^{-1})
C_{Ara} = arabinose concentration (g L^{-1})
C_{Et} = ethanol concentration (g L^{-1})
C_F = furfural concentration (g L^{-1})
$C_{F,crit}$ = critical furfural concentration causing complete inhibition of growth (g L^{-1})
C_{GA} = glucuronic acid concentration in lignocellulosic biomass (g kg^{-1})
C_G = glucose concentration (g L^{-1})
C_{HAc} = acetic acid concentration (g L^{-1})
C_{HMF} = 5-hydroxymethylfurfural concentration (g L^{-1})
C_{Ln} = lignin concentration in lignocellulosic biomass (g kg^{-1})
C_{SL} = acid soluble lignin concentration (g L^{-1})
C_{Xy} = xylose concentration (g L^{-1})
C_{Xn} = xylan concentration in lignocellulosic biomass (g kg^{-1})
C_x = biomass concentration (g L^{-1})
C_Z = cation Ca^{2+} concentration in detoxification (g L^{-1})
C_{Zj} = complex ion concentration in detoxification (g L^{-1})
E_i = activation energy for reaction i (J/mol)
h_f = starting time of finite element f
k_i = reaction rate constant for reaction i (min^{-1})
k_i^0 = frequency factor (min^{-1} wt $\%^{-n_i}$)
K_i = substrate inhibition constant (g L^{-1})
K_s = substrate limitation constant (g L^{-1})
M_{je} = number of data points collected for each measurement j in every experiment e
NE = number of experiments
NF = number of finite elements
NC = number of collocation points
n_i = order of reaction i with respect to acid concentration in Arrhenius equation
n_G = inhibiting factor for glucose (dimensionless)
P_i = threshold ethanol concentration (g L^{-1})
P_m = maximum ethanol concentration (g L^{-1})
$q_{p,max}$ = overall maximum specific ethanol production rate (g g^{-1} h^{-1})
$q_{s,max}$ = overall maximum specific substrate uptake rate (g g^{-1} h^{-1})
R = universal gas constant (8.3144 J/mol K)
T = temperature (K)
α = weighting factor for glucose consumption in cofermentation operation
μ_{max} = maximum specific growth rate of cells (h^{-1})
τ = normalized time in each finite element f
φ = basis function for Lagrange polynomial
ϕ = ratio of solid biomass to liquid in hydrolysis operation (g g^{-1})

REFERENCES

(1) Andersen, F. E.; Moreno, M. S.; Diaz, M. S. Model based optimization of bioethanol production from lignocellulosic biomass. Presented at the 2011 AIChE Annual Meeting, Oct 16−21, 2011, Minneapolis, MN, USA.

(2) Andersen, F. E.; Moreno, M. S.; Diaz, M. S. Dynamic modeling and parameter estimation for unit operations in lignocellulosic bioethanol. Presented at the 2012 AIChE Annual Meeting, Oct 28−Nov 2, 2012, Pittsburgh, PA, USA.

(3) Quintero, J. A.; Cardona, C. A. Process simulation of fuel ethanol production from lignocellulosics using Aspen Plus. *Ind. Eng. Chem. Res.* **2011**, *50*, 6205−6212.

(4) Martín, M.; Grossmann, I. E. Energy optimization of bioethanol production via hydrolysis of switchgrass. *AIChE J.* **2012**, *58*, 1538−1549.

(5) Mosier, N.; Wyman, C.; Dale, B.; Elander, R.; Lee, Y. Y.; Holtzapple, M.; Ladisch, M. Features of promising technologies for pretreatment of lignocellulosic biomass. *Bioresour. Technol.* **2005**, *96*, 673−686.

(6) Taherzadeh, M. J.; Karimi, K. Pretreatment of lignocellulosic wastes to improve ethanol and biogas production: A review. *Int. J. Mol. Sci.* **2008**, *9*, 1621−1651.
(7) Kumar, P.; Barrett, D. M.; Delwiche, M. J.; Stroeve, P. Methods for pretreatment of lignocellulosic biomass for efficient hydrolysis and biofuel production. *Ind. Eng. Chem. Res.* **2009**, *48*, 3713−3729.
(8) Talebnia, F.; Niklasson, C.; Taherzadeh, M. J. Ethanol production from glucose and dilute-acid hydrolyzates by encapsulated *S. cerevisiae*. *Biotechnol. Bioeng.* **2005**, *3*, 345−353.
(9) Zhang, S.; Marechal, F.; Gassner, M.; Périn-Levasseur, Z.; Qi, W.; Ren, Z.; Yan, Y.; Favrat, D. Process modeling and integration of fuel ethanol production from lignocellulosic biomass based on double acid hydrolysis. *Energy Fuels* **2009**, *23*, 1759−1765.
(10) Taherzadeh, M. J.; Eklund, R.; Gustafsson, L.; Niklasson, C.; Lidén, G. Characterization and fermentation of dilute-acid hydrolyzates from wood. *Ind. Eng. Chem. Res.* **1997**, *36*, 4659−4665.
(11) Pienkos, P. T.; Zhang, M. Role of pretreatment and conditioning processes on toxicity of lignocellulosic biomass hydrolysates. *Cellulose* **2009**, *16*, 743−762.
(12) Lavarack, B. P.; Griffin, G. J.; Rodman, D. The acid hydrolysis of sugarcane bagasse hemicelluloses to produce xylose, arabinose, glucose and other products. *Biomass Bioenergy* **2002**, *23*, 367−380.
(13) Purwadi, R.; Niklasson, C.; Taherzadeh, M. J. Kinetic study of detoxification of dilute-acid hydrolyzates by $Ca(OH)_2$. *J. Biotechnol.* **2004**, *114*, 187−198.
(14) Leksawasdi, N.; Joachimsthal, E. L.; Rogers, P. L. Mathematical modeling of ethanol production from glucose/xylose mixtures by recombinant Zymomonas mobilis. *Biotechnol. Lett.* **2001**, *23*, 1087−1093.
(15) Tjoa, I.; Biegler, L. T. Simultaneous solution and optimization strategies for parameter estimation of differential-algebraic equation systems. *Ind. Eng. Chem. Res.* **1991**, *30*, 376−385.
(16) Zavala, V. M.; Biegler, L. T. Large-scale parameter estimation in low-density polyethylene tubular reactors. *Comput. Chem. Eng.* **2006**, *45*, 7867−7881.
(17) Estrada, V.; Parodi, E. R.; Diaz, M. S. Determination of biogeochemical parameters in eutrophication models with simultaneous dynamic optimization approaches. *Comput. Chem. Eng.* **2009**, *33*, 1760−1769.
(18) Wächter, A.; Biegler, L. T. On the implementation of an interior-point filter line-search algorithm for large-scale nonlinear programming. *Math. Program.* **2006**, *106*, 25−57.
(19) Brooke, A.; Kendrick, D.; Meeraus, A.; Raman, R. *A User's Guide*; GAMS Development Corp., 2012. http://www.gams.com.
(20) Smets, I.; Bernaerts, K.; Sun, J.; Marchal, K.; Vanderleyden, J.; Van Impe, J. Sensitivity function-based model reduction. A bacterial gene expression case study. *Biotechnol. Bioeng.* **2000**, *80* (2), 195−200.
(21) Cassales, A.; Souza-Cruz, P. B.; Rech, R.; Ayub, M. A. Z. Optimization of soybean hull acid hydrolysis and its characterization as a potential substrate for bioprocessing. *Biomass Bioenergy* **2011**, *35*, 4675−4683.
(22) Gutierrez-Padilla, M. G. D.; Karim, M. N. Influence of furfural on the recombinant Zymomonas mobilis strain CP4 (pZB5) for ethanol production. *J. Am. Sci.* **2005**, *1*, 24−27.
(23) Biegler, L. T. *Nonlinear Programming: Concepts, Algorithms, and Applications to Chemical Processes*; Society for Industrial and Applied Mathematics: Philadelphia, PA, USA, 2010
(24) Holmberg, A.; Ranta, J. Procedures for parameter and state estimation of microbial growth process models. *Automatica* **1982**, *18* (2), 181−193.
(25) Biegler, L. T.; Zavala, V. M. Large-scale nonlinear programming using IPOPT: An integrating framework for enterprise-wide dynamic optimization. *Comput. Chem. Eng.* **2009**, *33*, 575−582.
(26) Bhatia, T.; Biegler, L. T. Dynamic optimization in the design and scheduling of multiproduct batch plants. *Ind. Eng. Chem. Res.* **1996**, *35*, 2234−2246.
(27) Biegler, L. T.; Cervantes, A. M.; Wächter, A. Advances in simultaneous strategies for dynamic process optimization. *Chem. Eng. Sci.* **2002**, *57*, 575−593.
(28) Aguilar, R.; Ramírez, J. A.; Garrote, G.; Vazquez, M. Kinetic study of the acid hydrolysis of sugar cane bagasse. *J. Food Eng.* **2002**, *55*, 309−318.
(29) Taherzadeh, M. J.; Karimi, K. Acid-based hydrolysis processes for ethanol from lignocellulosic materials: A review. *BioResources* **2007**, *2*, 472−499.
(30) Gírio, F. M.; Fonseca, C.; Carvalheiro, F.; Duarte, L. C.; Marques, S.; Bogel-Łukasik, R. Hemicelluloses for fuel ethanol: A review. *Bioresour. Technol.* **2010**, *101*, 4775−4800.
(31) Gurgel, L. V. A.; Marabezi, K.; Zanbom, M. D.; da Silva Curvelo, A. A. Dilute acid hydrolysis of sugar cane bagasse at high temperatures: A kinetic study of cellulose saccharification and glucose decomposition. Part I: sulfuric acid as the catalyst. *Ind. Eng. Chem. Res.* **2012**, *51*, 1173−1185.
(32) Lenihan, P.; Orozco, A.; O'Neill, E.; Ahmad, M. N. M.; Rooney, D. W.; Walker, G. M. Dilute acid hydrolysis of lignocellulosic biomass. *Chem. Eng. J.* **2010**, *156*, 395−403.
(33) Rahman, S. H. A.; Choudhury, J. P.; Ahmad, A. L. Production of xylose from oil palm empty fruit bunch fiber using sulfuric acid. *Biochem. Eng. J.* **2006**, *30*, 97−103.
(34) Saeman, J. F. Kinetics of wood saccharification. Hydrolysis of cellulose and decomposition of sugars in dilute acid at high temperature. *Ind. Eng. Chem.* **1945**, *37*, 43−52.
(35) Palmqvist, E.; Hahn-Hägerdal, B. Fermentation of lignocellulosic hydrolysates. II: inhibitors and mechanisms of inhibition. *Bioresour. Technol.* **2000**, *74*, 25−33.
(36) Martín, C.; Galbe, M.; Wahlbom, C. F.; Hahn-Hägerdal, B.; Jönsson, L. J. Ethanol production from enzymatic hydrolysates of sugarcane bagasse using recombinant xylose-utilising *Saccharomyces cerevisiae*. *Enzyme Microb. Technol.* **2002**, *31*, 274−282.
(37) Larsson, S.; Reimann, A.; Nilvebrant, N.-O.; Jönsson, L. J. Comparison of different methods for the detoxification of lignocellulose hydrolyzates of spruce. *Appl. Biochem. Biotechnol.* **1999**, *77*−*79*, 91−103.
(38) Martinez, A.; Rodriguez, M. E.; York, S. W.; Preston, J. F.; Ingram, L. O. Effects of $Ca(OH)_2$ treatments ("Overliming") on the composition and toxicity of bagasse hemicellulose hydrolysates. *Biotechnol. Bioeng.* **2000**, *69* (5), 527−536.
(39) Ranatunga, T. D.; Jervis, J.; Helm, R. F.; McMillan, J. D.; Wooley, R. J. The effect of overliming on the toxicity of dilute acid pretreated lignocellulosics: the role of inorganics, uronic acids and ether-soluble organics. *Enzyme Microb. Technol.* **2000**, *27*, 240−247.
(40) Horváth, I. S.; Taherzadeh, M. J.; Niklasson, C.; Lidén, G. Effects of furfural on anaerobic continuous cultivation of *Saccharomyces cerevisiae*. *Biotechnol. Bioeng.* **2001**, *75* (5), 540−549.
(41) Almeida, J. R. M.; Bertilsson, M.; Gorwa-Grauslund, M. F.; Gorsich, S.; Lidén, G. Metabolic effects of furaldehydes and impacts on biotechnological processes. *Appl. Microbiol. Biotechnol.* **2009**, *82*, 625−638.
(42) Balat, M. Production of bioethanol from lignocellulosic materials via the biochemical pathway: A review. *Energy Convers. Manage.* **2011**, *52*, 858−875.
(43) Chen, Y. Development and application of co-culture for ethanol production by co-fermentation of glucose and xylose: a systematic review. *J. Ind. Microbiol. Biotechnol.* **2011**, *38*, 581−597.
(44) Ranatunga, T. D.; Jervis, J.; Helm, R. F.; McMillan, J. D.; Hatzis, C. Identification of inhibitory components toxic toward *Zymomonas mobilis* CP4(pZB5) xylose fermentation. *Appl. Biochem. Biotechnol.* **1997**, *67*, 185−198.
(45) Krishnan, M. S.; Ho, N. W. Y.; Tsao, G. T. Fermentation kinetics of ethanol production from glucose and xylose by recombinant *Saccharomyces* 1400(pLNH33). *Appl. Biochem. Biotechnol.* **1999**, *77*−*79*, 373−388.
(46) Nakamura, Y.; Sawada, T.; Inoue, E. Mathematical model for ethanol production from mixed sugars by *Pichia stipitis*. *J. Chem. Technol. Biotechnol.* **2001**, *76*, 586−592.